2008

The Genome Sequence of the Metal-Mobilizing, Extremely Thermoacidophilic Archaeon *Metallosphaera sedula* Provides Insights into Bioleaching-Associated Metabolism

Kathryne S. Auernik
North Carolina State University

Yukari Maezato
University of Nebraska-Lincoln

Paul H. Blum
University of Nebraska - Lincoln, pblum1@unl.edu

Robert M. Kelly
North Carolina State University

APPLIED AND ENVIRONMENTAL MICROBIOLOGY, Feb. 2008, p. 682–692
0099-2240/08/$08.00+0 doi:10.1128/AEM.02019-07

Supporting information for this article is available following the references.

Vol. 74, No. 3

The Genome Sequence of the Metal-Mobilizing, Extremely Thermoacidophilic Archaeon *Metallosphaera sedula* Provides Insights into Bioleaching-Associated Metabolism▽†

Kathryne S. Auernik,[1] Yukari Maezato,[2] Paul H. Blum,[2] and Robert M. Kelly[1]*

Department of Chemical and Biomolecular Engineering, North Carolina State University, Raleigh, North Carolina 27695-7905,[1] *and Beadle Center for Genetics, University of Nebraska—Lincoln, Lincoln, Nebraska 68588-06662*[2]

Received 4 September 2007/Accepted 1 December 2007

Despite their taxonomic description, not all members of the order *Sulfolobales* are capable of oxidizing reduced sulfur species, which, in addition to iron oxidation, is a desirable trait of biomining microorganisms. However, the complete genome sequence of the extremely thermoacidophilic archaeon *Metallosphaera sedula* DSM 5348 (2.2 Mb, ~2,300 open reading frames [ORFs]) provides insights into biologically catalyzed metal sulfide oxidation. Comparative genomics was used to identify pathways and proteins involved (directly or indirectly) with bioleaching. As expected, the *M. sedula* genome contains genes related to autotrophic carbon fixation, metal tolerance, and adhesion. Also, terminal oxidase cluster organization indicates the presence of hybrid quinol-cytochrome oxidase complexes. Comparisons with the mesophilic biomining bacterium *Acidithiobacillus ferrooxidans* ATCC 23270 indicate that the *M. sedula* genome encodes at least one putative rusticyanin, involved in iron oxidation, and a putative tetrathionate hydrolase, implicated in sulfur oxidation. The *fox* gene cluster, involved in iron oxidation in the thermoacidophilic archaeon *Sulfolobus metallicus*, was also identified. These iron- and sulfur-oxidizing components are missing from genomes of nonleaching members of the *Sulfolobales*, such as *Sulfolobus solfataricus* P2 and *Sulfolobus acidocaldarius* DSM 639. Whole-genome transcriptional response analysis showed that 88 ORFs were up-regulated twofold or more in *M. sedula* upon addition of ferrous sulfate to yeast extract-based medium; these included genes for components of terminal oxidase clusters predicted to be involved with iron oxidation, as well as genes predicted to be involved with sulfur metabolism. Many hypothetical proteins were also differentially transcribed, indicating that aspects of the iron and sulfur metabolism of *M. sedula* remain to be identified and characterized.

Biomining exploits acidophilic microorganisms to recover valuable metals (i.e., Cu and Au) from ores (52, 56, 57, 59) in biohydrometallurgical processes conducted at temperatures ranging from ambient (44, 71) to 80°C (17). Higher-temperature operations involve consortia of extremely thermoacidophilic archaea from the genera *Sulfolobus*, *Acidianus*, and *Metallosphaera* (49, 50). For example, *Sulfolobus metallicus*, certain *Acidianus* species (12, 47), and *Metallosphaera sedula* (29, 33) all can mobilize metals from metal sulfides. However, not all members of these genera are metal bioleachers. In fact, the three *Sulfolobus* species with completed genome sequences (*S. solfataricus*, *S. acidocaldarius*, and *S. tokodaii*) are apparently unable to effect metal sulfide oxidation. Since genome sequences are not yet available for metal- bioleaching extreme thermoacidophiles, genetic features characteristic of this physiological capability remain to be seen.

Biomining is based upon biological oxidation of iron (Fe) and reduced inorganic sulfur compounds (RISCs). Two Fe(III)-driven chemical leaching mechanisms are catalyzed by microorganisms regenerating Fe(III) from Fe(II), facilitating release of valuable metals bound in metal sulfides (52, 56, 57, 59). As accumulation of precipitating RISC compounds can slow leaching rates (52), microbial RISC-oxidizing capabilities are beneficial. Extreme thermophiles are particularly desirable, as problematic passivation on ore surfaces decreases at higher temperatures. Since chemolithotrophs use Fe(II) and/or RISCs as energy sources, nutritional supplement costs are relatively low, thus minimizing process economic impact.

Components of electron transport chains involved in Fe and RISC oxidation are differentially expressed as a function of substrate in both meso- and thermoacidophilic bioleachers (5, 36, 55). Bacterial Fe oxidation studies focused on mesophilic *A. ferrooxidans* have shown that electrons from Fe(II) can be transported along either a "downhill" or an "uphill" electron pathway, towards a lower (O_2/H_2O)- or higher [$NAD(P)^+$/NAD(P)H]-potential redox couple, respectively (28). Both pathways involve electron transfer via cytochromes *c* and rusticyanin (Rus), a periplasmic blue copper protein (Bcp). The downhill and uphill pathways, encoded by the *rus* and *petI* operons, conclude with reduction of the final target by a cytochrome *c* oxidase (CoxABCD) and bc_1 complex (PetI), respectively, and are highly transcribed on Fe(II) relative to elemental sulfur (S^0) (7, 18, 72). In a proposed archaeal Fe oxidation model, based on *Ferroplasma* strains, the terminal oxidase combines select bc_1 complex-like and cytochrome *c* oxidase-like components and involves association of a Bcp, sulfocyanin (15). Aspects of this model were noted previously in the nonleacher *S. acidocaldarius* (39, 41), while a correlation between cytochromes *b*, $b_{558/562}$ (CbsAB), and Fe-S cluster proteins

* Corresponding author. Mailing address: Department of Chemical & Biomolecular Engineering, North Carolina State University, Raleigh, NC 27695-7905. Phone: (919) 515-6396. Fax: (919) 515-3465. E-mail: rmkelly@eos.ncsu.edu.

† Supplemental material for this article may be found at http://aem.asm.org/.

▽ Published ahead of print on 14 December 2007.

(possible quinol oxidase components) and the bc_1 complex has been proposed (27, 39, 65, 75). Finally, a gene cluster containing terminal oxidase and electron transport chain components, highly transcribed on Fe(II) versus S^0, was identified in *S. metallicus* (5).

Extremely thermoacidophilic archaeal RISC oxidation mechanisms have not been established. RISC electrons may enter the electron transport chain via a membrane-bound thiosulfate ($S_2O_3^{2-}$):quinone oxidoreductase (TQO), a sulfite:acceptor oxidoreductase, or possibly a sulfide:quinone oxidoreductase (38). Despite the annotation, tetrathionate hydrolases (TetH) expressed on S^0, FeS_2, and $S_2O_3^{2-}$ substrates have been noted in *A. ferrooxidans* and *Acidithiobacillus caldus* (8, 35, 61). Certain terminal oxidase components have been expressed in extremely thermoacidophilic archaea grown on specific RISCs (36, 54). Although not directly linked to electron transport, sulfur oxygenase reductases (Sor) are believed to be important for breakdown of intracellular RISCs, particularly S^0 or polysulfides (11, 37, 69). *M. sedula* growth on S^0 and metal sulfides (i.e., FeS_2 and chalcopyrite [$CuFeS_2$]), has been documented (29). With $S_2O_3^{2-}$ as a primary intermediate of acid-insoluble metal sulfide leaching, this may be a RISC substrate. However, there are no reports of *M. sedula* growth on $S_2O_3^{2-}$ or other RISCs, such as sulfite (SO_3^{2-}) or polythionates.

Although *M. sedula* presumably grows mixotrophically, autotrophy is critical in biomining environments, where relatively small amounts of organic carbon are available. Several members of the *Sulfolobales*, including *M. sedula*, purportedly fix carbon (CO_2) via a modified 3-hydroxypropionate cycle, identified in *Chloroflexus aurantiacus* (31–34, 43, 67). In *M. sedula*, two enzymes of this cycle have been characterized biochemically (1, 33), while two additional enzymes' activities were detected in autotrophically grown cell extracts, suggesting their involvement in CO_2 fixation (32).

Heavy metals, typically toxic at concentrations higher than trace amounts, are routinely encountered by biomining acidophiles. In contrast to the substantial amount of information about metal toxicity in neutrophiles (48), relatively little is known about such mechanisms in acidophiles, despite their higher resistance levels (16). Toxicity and mechanisms of resistance to mercury (Hg) have been investigated in *S. solfataricus* (14, 63, 64), while possible copper (Cu) resistance mechanisms have been studied in *S. solfataricus* and *S. metallicus* (19, 58). Continued study of heavy metal toxicity and resistance mechanisms in bioleachers is important, especially for cases like *M. sedula*, where tolerance to some metals, particularly Cu, may require improvement to make it competitive with other microbial biominers, such as *S. metallicus* and *A. ferrooxidans* (16, 30, 58).

Adhesion mechanisms of biomining microorganisms to acid-insoluble metal sulfides or S^0 may be important to oxidation rates. Study of bioleachers' extracellular polymeric substances, often exopolysaccharides (EPS), has centered on *A. ferrooxidans* (6, 13, 23, 24, 51, 62). EPS production, composition, and properties were all observed to be a function of growth substrate in *A. ferrooxidans* (23, 24). In addition, significant homology between the components of the bacterial type II secretion, type IV pilus, and archaeal flagellar (Fla) systems has been suggested (53). Bacterial type IV pili and Fla systems have been implicated in adhesion (46, 66), and pilus-like structures, along with "wiggling of the cells at the ore," were observed during initial characterization of *M. sedula* (29).

To better understand the defining features of extreme thermoacidophiles capable of metal sulfide oxidation, the genome sequence of *M. sedula* was completed and probed for clues with respect to five physiological areas (iron oxidation, sulfur oxidation, carbon fixation, metal toxicity, and adhesion) that are important to its current and future role in biomining operations. In addition, whole-genome transcriptional response analysis was used to identify specific open reading frames (ORFs) related to Fe oxidation.

MATERIALS AND METHODS

Sequencing of the *M. sedula* genome. *M. sedula* (DSM 5348T) was purified to clonality by aerobic cultivation at 70°C on a solid medium, prepared as described previously (64), and adjusted to a pH of 2.5 with sulfuric acid. High-molecular-weight genomic DNA was isolated, as described previously (26), and provided to the U.S. Department of Energy Joint Genome Institute (http://www.jgi.doe.gov/) for cloning and shotgun sequencing. A combination of small (average insert sizes, 3 and 8 kb) and large (40 kb, fosmid) insert libraries were prepared and used for analysis as indicated at http://www.jgi.doe.gov/.

Annotation. Critica, Generation, and Glimmer software programs were used for coding region detection and gene identification. TMHMM 2.0 (http://www.cbs.dtu.dk/services/TMHMM/) was used to predict transmembrane helices in translated sequences. SignalP v2.0b2 (http://www.cbs.dtu.dk/services/SignalP-2.0/) was used to predict the presence and location of N-terminal signal peptides.

Comparative analysis. For comparative genomics, *M. sedula* gene sequences and annotations were downloaded from the JGI microbial genome website (http://genome.ornl.gov/microbial/msed/28feb07/). Other sequences referenced were obtained from GenBank, with the exception of *A. ferrooxidans* ATCC 23270 sequences, which were obtained from The Institute for Genome Research's Comprehensive Microbial Resource. Basic Local Alignment Search Tool (BLAST) searches were conducted using a BLOSUM62 matrix with either the NCBI protein-protein BLAST program (BLASTP) against the Swissprot or nr database or the ORNL Microbial BLAST server's BLASTP program against the Msed database. "Significant similarity" or "significant homology" was defined as $\geq$20% identity and an Eval value of $\leq 10^{-5}$, unless otherwise noted.

Electron microscopy. Samples used for scanning electron microscopy were grown aerobically at 70°C in a minimal salts medium (60) containing 0.1% FeS_2 as the sole energy source; prior to use, the FeS_2 was sterilized by baking for 3 days at 140°C. Glutaraldehyde-fixed cells treated with osmium tetroxide were applied to poly-L-lysine-coated, gold-palladium-treated coverslips, followed by ethanol dehydration. Following critical-point drying, gold-palladium-coated cells were visualized with a Hitachi S-3000N variable pressure scanning electron microscope (http://bsweb.unl.edu/labs/blum/index.html).

Transcriptional response analysis. An oligonucleotide microarray was developed using a minimum of one 60-mer probe (designed using OligoArray 2.1 software, synthesized by Integrated DNA Technologies) for each identifiable protein-encoding ORF in the *M. sedula* genome. Cells (DSMZ 5348) were grown aerobically at 70°C in an orbital shaking oil bath at 70 rpm on DSMZ 88 medium (pH 2), supplemented with 0.1% yeast extract (YE). An initial density of mid-10^6 cells/ml was used in four 1-liter bottles containing 300 ml of the same medium. Approximately 7.5 g/liter of $FeSO_4 \cdot 7H_2O$ was added to two of these cultures prior to inoculation. At harvest, cultures in mid-exponential phase (~24 h of growth, mid-10^7 cells/ml) were quickly chilled and then centrifuged at 9,510 $\times$ *g* for 15 min at 4°C. RNA was extracted and purified (RNAqueous; Ambion), reverse transcribed (Superscript III, Invitrogen), repurified, labeled with either Cy3 or Cy5 dye (GE Healthcare), and hybridized to one of two microarray slides (Corning). Slides were scanned on a Perkin-Elmer scanner, and raw intensities were quantitated with ScanArray Express 2.1 software. Normalization of data and statistical analysis were performed using JMP Genomics 6.0.2 software (SAS Institute, Cary, NC).

Nucleotide sequence accession number. The 18 contigs of the draft genome sequence were made available publicly on 27 November 2006, with the final assembly released on 25 April 2007 and listed under GenBank accession no. CP000682 (http://genome.jgi-psf.org/finished_microbes/metse/metse.info.html).

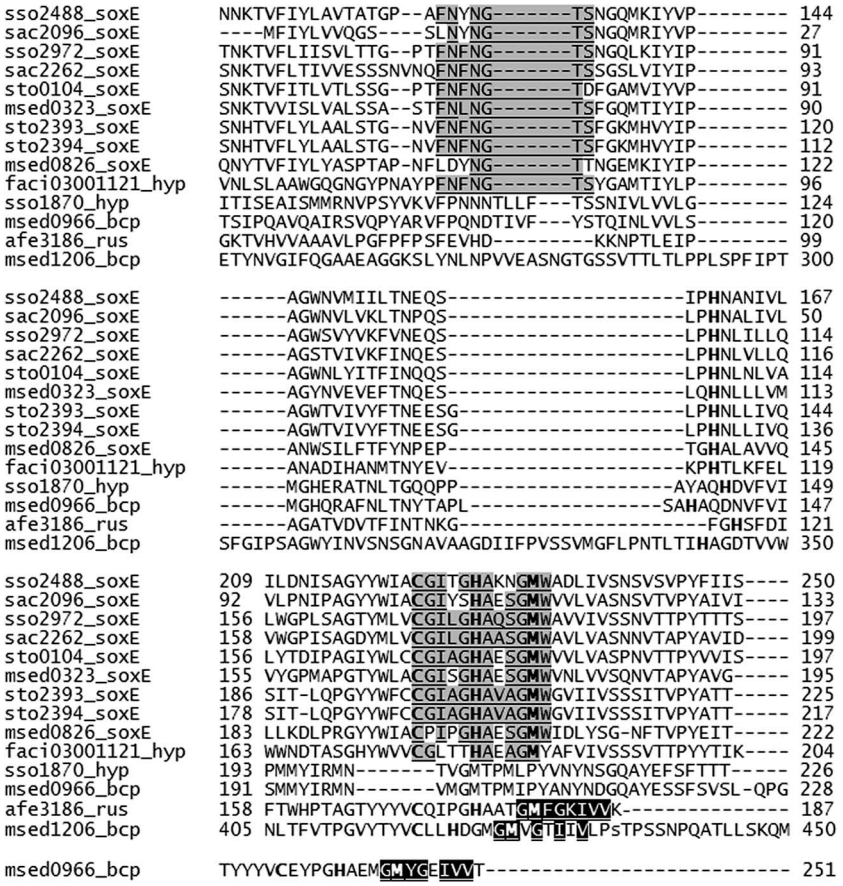

FIG. 1. Selected sections of a full multiple-sequence alignment of known and putative proteins involved in Fe oxidation performed by CLUSTAL W (1.83). Amino acids known or predicted to be involved with copper binding (4, 10, 25, 76) are shown in bold. Segments underlined and highlighted in gray and black show protein signatures for sulfocyanin and rusticyanin, respectively, with intermediate nonhighlighted amino acids failing to meet currently recognized positional consensus amino acids (25). Abbreviations: sso, *S. solfataricus*; sac, *S. acidocaldarius*; sto, *S. tokodaii*; msed, *M. sedula*; faci, *F. acidarmanus*; afe, *A. ferrooxidans*; soxE, sulfocyanin; hyp, hypothetical protein; bcp, blue copper protein; rus, rusticyanin.

RESULTS AND DISCUSSION

Organization and general features of the genome. The *M. sedula* genome (46% G+C) encodes 2,258 proteins, 35% of which are annotated as either "hypothetical protein" or "protein of unknown function." However, almost 90% of these have their strongest similarity ("top hit") to *Sulfolobus* species (786 to *S. solfataricus*, 829 to *S. tokodaii*, 327 to *S. acidocaldarius*, 14 to "*S. islandicus*," and 3 to *S. shibatae*), with 35 ORFs being most similar to genes in *Acidianus* species. This raises some interesting questions. Will the genes responsible for the biomining capabilities of *M. sedula* be found within the 10% of gene sequences with strongest similarities to non-*Sulfolobales* or nonarchaeal microorganisms? Or, conversely, will subtle differences in the *Sulfolobales*' gene sequences result in the distinction between thermoacidophilic leachers and nonleachers?

Iron oxidation. The Fe oxidation mechanism in *M. sedula* is, as yet, unknown. The organization and composition of at least five respiratory clusters found in the genome sequence, two of which are predicted to be highly transcribed during growth on Fe(II) or FeS_2, differ from those of the bacterial *rus* and *pet* operons. No PetC-like ORFs (cytochrome *c* subunit of the bc_1 complex) are apparent. This is consistent with reports that archaeal genomes of *Ferroplasma* and *Sulfolobus* species do not contain cytochromes *c* (68) and suggests that acidophilic archaeal and bacterial Fe oxidation do not occur via the same mechanism. The gene neighborhood organization of respiratory clusters in *M. sedula* provides support for the *Ferroplasma* hybrid terminal oxidase model.

Genes for four Bcp-like proteins are found in the genome; two are annotated as hypothetical sulfocyanins (SoxE). Figure 1 displays a multiple-sequence alignment of these Bcps, along with similar Bcp-like sequences from other microorganisms. Almost all the Bcp sequences appear to contain four ligands important for Cu binding and the characteristically high positive redox potential of Rus in *A. ferrooxidans* (4, 76). Both Msed0323 and Msed0826 contain two recognized protein signatures for sulfocyanins, while the two remaining Bcps from *M. sedula* (Msed0966 and Msed1206) contain rusticyanin protein signatures (25). The SoxE-like sequences appear to align fairly well with each other, but the same cannot be said for the Rus-like sequences. The relevance of poor alignment between Rus-like sequences to protein function is not clear. The archaeal Rus-like proteins cannot have the same cellular location

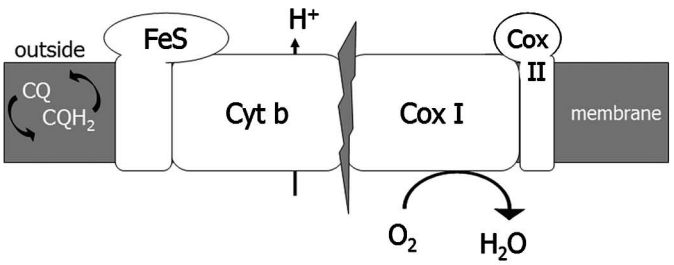

Locus	SoxL/F	SoxC/G/N	SoxB/M	SoxA/H	Source (organism)
1	Msed0288	Msed0291	Msed0290	Msed0289	Lubben 1994 Sac (SoxABCD)
2	Msed0322	Msed0321	Msed0324	Msed0320	Castresana 1995 Sac (SoxFGHM)
3	Msed0501	Msed0500			Hiller 2003 Sac (SoxNL)
4			Msed0484-5	Msed0480	Bathe 2007 Sme, Sto (SoxHB)
5			Msed2032	Msed2031	Purschke 1997 Aam (DoxBC)

FIG. 2. Proposed organization of common elements in terminal oxidase complexes of *M. sedula*. Terminal oxidase complexes have been proposed to be hybrids of bacterial bc_1 complexes, containing Fe-S Rieske (SoxL or SoxF) and cytochrome *b* (SoxC, SoxG, or SoxN) components, and cytochrome oxidases, containing Cox subunits I and II (SoxB or SoxM and SoxA or SoxH, respectively). Also provided is the relative genome sequence location (ORF numbers) of these common elements; previous studies of these general subunit or cluster functions are listed at the far right. Sac, *S. acidarmanus*; Sme, *S. metallicus*; Sto, *S. tokodaii*; Aam, *A. ambivalens.*

as their bacterial periplasmic counterpart. The Msed0966 product is more similar to the Rus found in *A. ferrooxidans* (Afe3186) than that of Msed1206. Both have predicted N-terminal signal peptides, but the Msed1206 protein also contains a single, predicted C-terminal hydrophobic transmembrane region. Although the other sequenced *Sulfolobus* species contain multiple SoxE homologs, only *S. solfataricus* (Sso1870) appears to contain a Rus-like (Msed0966-like) sequence. However, Sso1870 does not appear to contain a recognized Rus protein signature or the four ligands noted as important to Cu binding and redox potential.

Three sets of ORFs with low similarity to the PetAB subunits of the bc_1 complex are found in the *M. sedula* genome (Msed0288 and Msed0291, Msed0322 and Msed0321, and Msed0501 and Msed0500) (Fig. 2). In each case, a Rieske protein (SoxL/SoxF) pairs with a cytochrome *b* (SoxC/SoxG/SoxN). In the first two cases, the Rieske protein and cytochrome *b* are clustered with cytochrome oxidase (Cox) subunits I and II (SoxAB or SoxHM) at the same loci, suggesting close association between quinol- and Cox-like subunits. In the case of locus 3, there is another Cox I-Cox II pair located further downstream (locus 4) which lacks a corresponding Rieske-cytochrome *b* (PetAB-like) pair. However, it is not clear if loci 3 and 4 should be grouped into a single, more diffuse, locus. Both loci contain a cytochrome $b_{558/562}$ (CbsAB; Msed0503 and -0504 and Msed0477 and -0478). Limited information available makes it difficult to determine whether CbsAB could substitute for quinol oxidase or Cox components of a terminal oxidase; however, previous studies have suggested that CbsAB may play a role in extracellular electron transport similar to that of the bc_1 complex (27, 65, 75). Locus 5 encodes DoxBCE (Msed2030 to Msed2032), the SoxAB-like terminal oxidase components from *Acidianus ambivalens*, and appears to be missing quinol oxidase-like subunits. Interestingly, Msed1191 appears to encode a lone quinol oxidase fusion protein (cytochrome *b* N-terminal region and Rieske protein C-terminal region).

Because locus 1 *soxB* (Msed0290) was reported to be up-regulated on S^0, compared to FeS_2 or YE (36), and DoxBCE expression and copurification with TQO subunits (DoxDA) were noted under S^0-oxidizing conditions in *A. ambivalens* (45, 54), it seems likely that the locus 1 and 5 respiratory clusters in *M. sedula* would also be stimulated during growth on RISCs. Locus 2 *soxM* (Msed0324) was reported as being up-regulated on YE, compared to FeS_2 or S^0 (36). Locus 3 *cbsA* (Msed0504) was found to have higher rates of transcription on FeS_2 than YE or S^0 (36); therefore, the entire locus is predicted to be up-regulated on Fe(II). Interestingly, locus 3 follows a proton efflux ATPase (Msed0505). Previous *A. ferrooxidans* studies suggested that this type of ATPase could function in either direction to regulate a cytochrome oxidase on the basis of available ATP, restoring proton motive force or supporting NADP(H) reduction (18). Locus 4 contains a gene cluster with homology to *fox* genes in *S. tokodaii* and *S. metallicus*, which were demonstrated to be up-regulated on Fe(II) versus S^0 (5). While locus 3 components appear to be present in both *S. acidocaldarius* and *S. solfataricus* genomes (27, 65), neither genome contains *fox* homologs (excepting FoxHJ in *S. solfataricus* and FoxH in *S. acidocaldarius*). This is not entirely surprising, as neither organism appears to be capable of growth on Fe(II). In light of this observation, the *fox* gene cluster is likely essential for metal mobilization. Because *S. tokodaii* was

recently reported to grow on Fe(II) (5) and its genome does not seem to encode Rus, it is not clear whether rusticyanin is essential for archaeal Fe oxidation or whether an alternative redox protein, such as sulfocyanin (SoxE), may perform an equivalent function. It is interesting that locus 4 includes a gene for a Cox II homolog (*soxH*; Msed0480) which contains conserved Cu-binding ligands similar to locus 2 SoxH (Msed0320) of the SoxM supercomplex, which is thought to interact with sulfocyanin (Msed0323), also of the SoxM supercomplex (39). Taking these data together, the predicted Fe oxidation capacity encoded in locus 4 could involve sulfocyanin, rusticyanin, or both. Because Msed1191 is unique to the BLAST database (as of September 2007), no similar sequence could be identified to predict what type of substrate could induce transcription of this ORF.

Sulfur oxidation. *M. sedula* encodes a pair of proteins (Msed0363 and Msed0364) with significant similarity to DoxDA subunits of the TQO in *A. ambivalens* (45). At least two sulfite:acceptor oxidoreductase-like proteins exist in *M. sedula*: a putative sulfite oxidase (Msed0362) on the strand opposite *doxDA* and an *A. ferrooxidans* CysI-like (Afe3210) putative sulfite reductase (Msed0961) near a putative rusticyanin; however, neither appears to be membrane associated. Of the five ORFs in *M. sedula* (Msed0353, -0558, -1039, -1323, and -2059) with significant similarity to putative sulfide:quinone oxidoreductase proteins in *A. ferrooxidans* (Afe1293 and Afe2761), only Msed1039 is predicted to contain a signal peptide. The *M. sedula* genome encodes a membrane-associated protein (Msed0804) with significant similarity to TetH found in both *A. ferrooxidans* (Afe2996) and *Acidithiobacillus caldus* (ABP38225). No counterparts can be identified in either *S. solfataricus* or *S. acidocaldarius*, although Sto1164 appears to be similar to the TetH of *A. ferrooxidans.* Neither an archaeal nor a bacterial Sor sequence is evident in the genome of *M. sedula*. While Sor is also apparently absent from the genomes of *S. solfataricus* and *S. acidocaldarius*, it is present in *S. tokodaii* and "*F. acidarmanus*."

Putative versions of genes for adenosine phosphosulfate (APS) reductase and sulfate adenylyl transferase (SAT) are colocated in *M. sedula* (Msed0962 and Msed0963), on the strand opposite a putative sulfite reductase gene (Msed0961). Depending on operational direction, these proteins could link RISCs to substrate-level phosphorylation. Operating oxidatively, as seen in chemolithotrophs, APS "reductase" converts SO_3^{2-} to APS, followed by SAT oxidation of APS to sulfate and ATP (74). Operating reductively, as seen in heterotrophs and autotrophs, requires function of SAT and then APS reductase, converting sulfate to SO_3^{2-}. A sulfite reductase further reduces SO_3^{2-} to sulfide, and then cysteine is formed via an *o*-acetyl-L-serine(thiol) lyase (70) or a cysteine synthase. Similar to *M. sedula*, the *A. ferrooxidans* 23270 genome also encodes a collocated APS-SAT pair, although the SAT sequence does not appear to be similar to that of *M. sedula*. SAT is usually encoded by two genes, one for an ATP sulfurylase and one for an APS kinase, although there are instances of their fusion (74). However, in *M. sedula*, only the ATP sulfurylase component is found, suggesting that APS, and not phosphoadenosine phosphosulfate, is formed. This is supported by the APS reductase sequence, which contains four cysteines (for 4Fe-4S center coordination) characteristic of APS reductase but missing in phosphoadenosine phosphosulfate reductase (70). Similarly, the CysI-like sulfite oxidoreductase subunit (Msed0961) is found in *A. ferrooxidans*, along with a flavoprotein subunit (CysJ) (70); however, in *M. sedula*, the CysJ-like component appears to be absent. Because the APS-SAT pair appears in nonleaching *Sulfolobus* species, the importance of these proteins in a bioleaching microorganism is unclear.

Finally, one putative rusticyanin mentioned previously (Msed0966) is located on the strand opposite of the APS-SAT pair in *M. sedula*. The clustering of this gene relative to those involved with sulfur metabolism may be coincidental; however, it may also suggest a physiological link between Fe and RISC oxidation important for bioleaching. Preliminary support for this hypothesis is based on an *A. ferrooxidans* study, which showed rusticyanin to be up-regulated during early exponential growth phase on a sulfur substrate (55).

Carbon metabolism. Sequences of genes for the two previously characterized enzymes of the 3-hydroxypropionate cycle (catalyzing steps 1, 2, and 4) can be located in the genome (Fig. 3). Potential sequences of genes for previously detected enzymatic activities of propionyl coenzyme A (propionyl-CoA) synthase (step 3) and fumarate hydratase (step 9) activities were also found. Although no propionyl-CoA synthase gene is annotated in the *M. sedula* genome, there are multiple AMP-dependent synthetase/ligase candidates, with Msed1353 having the most sequence similarity to the N-terminal propionyl-CoA synthases from both *C. aurantiacus* (AAL47820) and *Roseiflexus* RS-1 (YP_001277513) (20). It is interesting that both bacterial enzymes are two to three times the size of the Msed1353 protein, which raises the prospect that a multisubunit propionyl-CoA synthase complex exists in *M. sedula*. Querying amino acids ~900 to 1100 and ~1300 to 1500 of both bacterial enzymes against the *M. sedula* genome results in hits to ORFs automatically annotated as enoyl-CoA hydratases (or 3-hydroxybutaryl-CoA dehydratases) and alcohol dehydrogenases, respectively. Two classes of fumarate dehydratase were also identified (Msed1115 and Msed1116, class I; Msed1462, class II). Candidates for the six additional enzymatic steps (steps 5, 6, 8, 10, 11, and 14) of the cycle can be identified in the genome sequence, with the predicted assignment of Msed0381 to steps 10, 11, and 14 based on its sequence similarity to the gene for the single enzyme in *C. aurantiacus* (*mcl*) responsible for malyl-, β-methylmalyl-, and *S*-citramalyl-CoA lyase activity (20, 42). Recent information suggests that at least part of the pathways in *C. aurantiacus* and *M. sedula* evolved independently (1). Hence, it is not surprising to find that the genome is devoid of sequences with similarity to encoded enzymes responsible for transferase activity in *C. aurantiacus* (21, 22) (steps 7 and 10). Because components of this pathway identified in *M. sedula* are not clustered, genome location is of limited use in determining the remaining enzymes participating in the pathway.

Metal tolerance. Microbial P-type ATPases, specifically CPX (Cys-Pro-X)-ATPase, have been proposed to mediate efflux of heavy metal cations, such as Cu, Zn, and Cd (16, 48, 58). A CPX-ATPase has been identified in *M. sedula* (Msed0490), with a C-P-C (Cys-Pro-Cys) pattern located in the fifth of seven predicted transmembrane regions. This gene has significant homology to a P-type ATPase in *S. solfataricus* (CopA) implicated in Cu(II), and possibly also cadmium, cat-

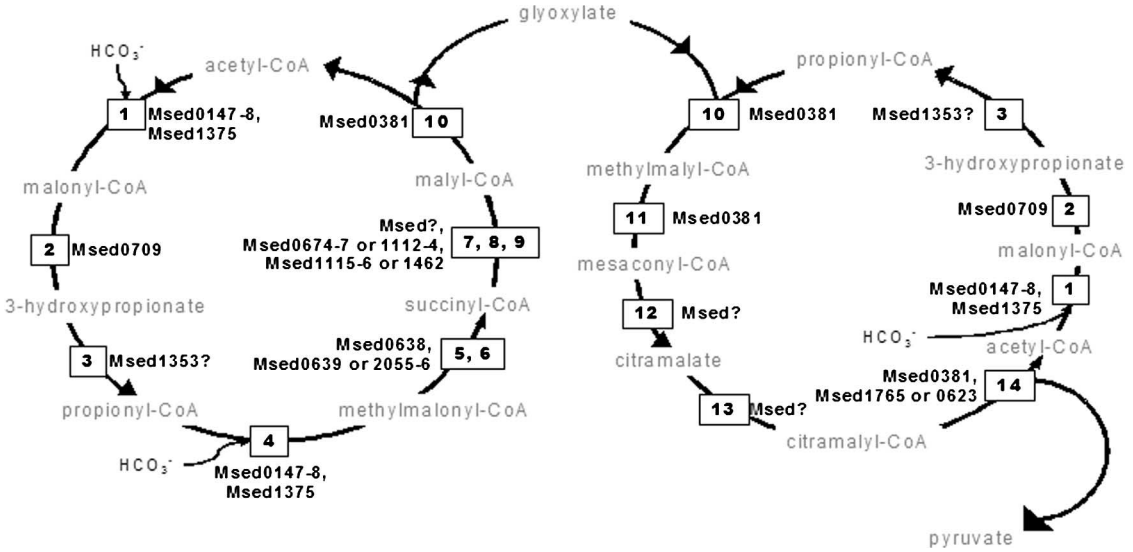

FIG. 3. The 3-hydroxypropionate cycle that is thought to operate in *C. aurantiacus* (adapted from references 20 and 21). ORF numbers predicted to encode the required enzymes are as follows: 1, acetyl-CoA carboxylase; 2, malonyl-CoA reductase; 3, propionyl-CoA synthase; 4, propionyl-CoA carboxylase; 5, methylmalonyl-CoA epimerase; 6, methylmalonyl-CoA mutase; 7, succinyl-CoA:L-malyl-CoA transferase; 8, succinate dehydrogenase; 9, fumarate dehydratase; 10, L-malyl-CoA lyase; 11, β-methylmalyl-CoA lyase; 12, unknown enzymes; 13, succinyl-CoA: citramalate-CoA transferase; 14, *S*/*R*-citramalyl-CoA lyase.

ion efflux (19). Ettema et al. (19) demonstrated that the metal efflux process involved a metallochaperone (CopM) having a 32-bp overlap with CopA and a new type of archaeal transcriptional regulator (CopT). *M. sedula* contains ORFs with significant similarity to both CopM and CopT (Msed0491 and Msed0492). However, the *copMA* overlap is limited to 10 bp, and the location of *copT* (on the opposite strand) makes the gene organization reminiscent of versions in the *S. tokodaii* and *S. acidocaldarius* genomes.

With respect to the polyphosphate mechanism proposed for Cu(II) detoxification in *S. metallicus* (58), Msed0740 is annotated as a probable polyphosphate/NAD kinase (*ppnk*), and Msed0981 has 37% similarity to the Ppx previously characterized in *S. solfataricus* (9). Searching for possible metal-phosphate complex exporters, no significant hits to *E. coli* phosphate transport systems (PstSCAB or Pit) were identified in *M. sedula*. However, as found with other genome-sequenced acidophiles (2, 58), use of an *S. cerevisiae* Pho84 sequence query produced results: three hits with similarities of 25 to 30% (Msed1512, Msed1094, and Msed0866). Using the top Pho84-like sequence in *A. ferrooxidans* (Afe0861) as a template, four hits with similarities of 30 to 32% resulted (the previous three plus Msed0846). All four hits belong to the major facilitator superfamily of substrate transporters. Msed1521 encodes a hypothetical protein downstream of Msed1512 with weak similarity to a phosphate transport regulation protein (COG1392, PFAM01865). Msed1968 (COG0704) encodes a putative phosphate uptake regulator.

A gene corresponding to an arsenite transporter (ArsB) was also identified (Msed2086; COG1055). The As(III) membrane potential-driven pump is typically found along with a repressor protein (ArsR) and sometimes with an As(V) reductase (ArsC), an As resistance-boosting APTase (ArsA), and/or a secondary regulation protein (ArsD) (16). In *M. sedula*, however, ArsB appears to stand alone. Msed1005 potentially encodes an ArsR-like regulatory protein with a TRASH domain, but it is unclear whether this protein might be involved in the regulation of ArsB, MerAH (Msed1241 and Msed1242), or some other metal resistance mechanism.

Adhesion. Figure 4 depicts *M. sedula* attached to FeS_2 and apparent EPS production. In support of this observation, the Msed1805-1857 locus encodes proteins potentially involved in EPS production. Queries from *A. ferrooxidans* (Afe1738) and *Vibrio cholerae* (Vps21) produced hits with significant similarity to Msed1810. All three sequences are annotated as a UDP-glucose (or mannose) 6-dehydrogenase (EC 1.1.22). Msed1809, which shares a 3-bp overlap with Msed1810, has lower, but significant, similarity to Afe1739, although both sequences are

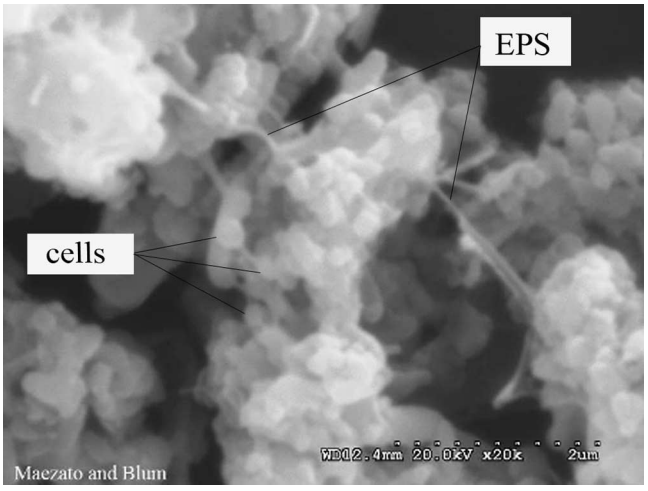

FIG. 4. *M. sedula* attached to a FeS_2 substrate. Bar, 2 μm.

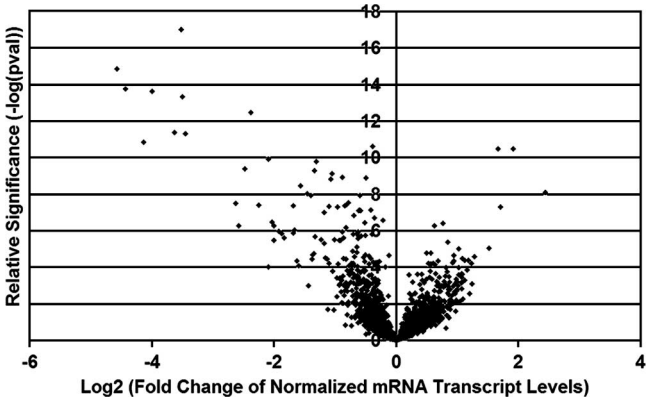

FIG. 5. Volcano plot of *M. sedula* microarray dye-flip results (YE versus YE+$FeSO_4$). Negative *x*-axis values represent ORFs more highly transcribed on YE+$FeSO_4$ while positive *x*-axis values represent ORFs more highly transcribed on YE alone. As points of reference on the *y* axis, *P* values of 0.05, 5×10^{-5}, and 5×10^{-10} correspond to significance values of 1.3, 4.3, and 9.3, respectively.

annotated as encoding UDP glucose 4-epimerase. The Msed1808 protein, annotated as a hypothetical protein, shares significant similarity with glycosyltransferases of *Staphylococcus aureus* (CapM) and *V. cholerae* (Vps32) implicated in capsular polysaccharide biosynthesis (40, 73). Msed1811, annotated as encoding a UDP-glucose pyrophosphorylase (EC 2.7.7.9), is not related to the EPS query sequences used, but, like Msed1808-10, it may encode enzymes involved in the synthesis of biofilm components, specifically glucuronic acid via the Leloir pathway (3). EPS of $FeSO_4$- and FeS_2-grown cells of *A. ferrooxidans* contain Fe(III) complexed with glucuronic acid, which is believed to impart an overall positive charge to the EPS, promoting attachment to FeS_2, which tends to maintain an overall negative charge at low pH (62). Additional ORFs located further downstream in this 1800s region have annotations suggestive of a role in formation of other EPS components (i.e., UDP-galactose, dTDP-rhamnose), but specific biochemical functions and cellular roles of the encoded proteins remain to be seen.

Genome analysis reveals at least four gene clusters with similarities to the type II/IV/Fla systems. Msed1324 to Msed1330 appear to encode seven flagellar proteins. The Msed1324 protein, annotated as FlaJ, contains eight predicted transmembrane regions and shares a 14-bp overlap with Msed1325. Msed1325 and Msed1326 (FlaIH) encode two cytoplasmic subunits related to ATPases (COG0630 and COG2874), while Msed1327 to Msed1329 overlap each other by 1 bp (Msed1327 and Msed1328) or 23 bp (Msed1328 and Msed1329) and are all predicted to have one N-terminal transmembrane helix. Msed1327 and Msed1328 correspond to FlaFG, while the Msed1329 protein shares no identity with characterized proteins. Msed1330 is annotated as encoding a flagellin protein and has similarity to the major preflagellin/prepilin FlaB genes (COG1681). Outside of this cluster, there are at least three other pairs of FlaIJ-like protein genes

TABLE 1. Transcriptional response of YE-grown *M. sedula* to ferrous sulfate

Bioleaching characteristic	Msed ORF	GenBank annotation	Change (fold): YE+$FeSO_4$ vs YE	Significance[a] ($\log_{10}$ *P* value)	Annotation
Iron oxidation (locus 4)	0477	Hypothetical	1.8 ↓	2.6	Putative *cbsB*/*foxD*
	0478	Hypothetical	3.3 ↓	7.3	Putative *cbsA*/*foxC*
	0479	Hypothetical	5.4 ↓	8.0	Hypothetical protein
	0480	Cytochrome *c* oxidase (subunit II)	3.8 ↓	10.5	Putative cytochrome oxidase (*soxH*/*foxB*)
	0484	Cytochrome *c* oxidase (subunit I)	1.8 ↑	4.5	Putative cytochrome oxidase (*soxB*/*foxA*)
Iron oxidation (locus 3)	0500	Cytochrome b/b_6, N-terminal domain	3.0 ↑	4.1	Putative quinol oxidase (*soxN*)
	0501	Rieske (2Fe-2S) domain	1.9 ↑	3.0	Putative quinol oxidase (*soxL*)
	0503	Hypothetical	1.7 ↑	3.6	Putative *cbsB*
	0504	Hypothetical	2.0 ↑	1.7	Putative *cbsA*
Sulfur metabolism	0960	Uroporphyrin-III C/tetrapyrrole (corrin/porphyrin) methyltransferase	2.5 ↑	9.3	Putative uroporphyrin III C-methyltransferase
	0961	Nitrite and sulfite reductase 4Fe-4S region	2.9 ↑	8.5	Putative sulfite reductase
	0962	Adenylylsulfate reductase, thioredoxin dependent	3.2 ↑	5.9	APS reductase
	0963	Sulfate adenylyltransferase	1.9 ↑	3.1	Sulfate adenylyltransferase
Iron oxidation	1191	Rieske (2Fe-2S) domain	4.3 ↑	4.0	Putative quinol oxidase fusion (*soxN-soxL*)
Adhesion	1197	Type II secretion system protein E	12.4 ↑	11.4	Putative ATPase (*fla*I)
	1198	Type II secretion system protein	6.0 ↑	6.3	Putative *fla*J
Iron oxidation	1206	Blue (type 1) copper domain	1.8 ↑	4.4	Putative rusticyanin

[a] For reference, significance values of 1.3, 4.3, and 9.3 correlate to *P* values of 0.05, 5×10^{-5}, and 5×10^{-10}, respectively.

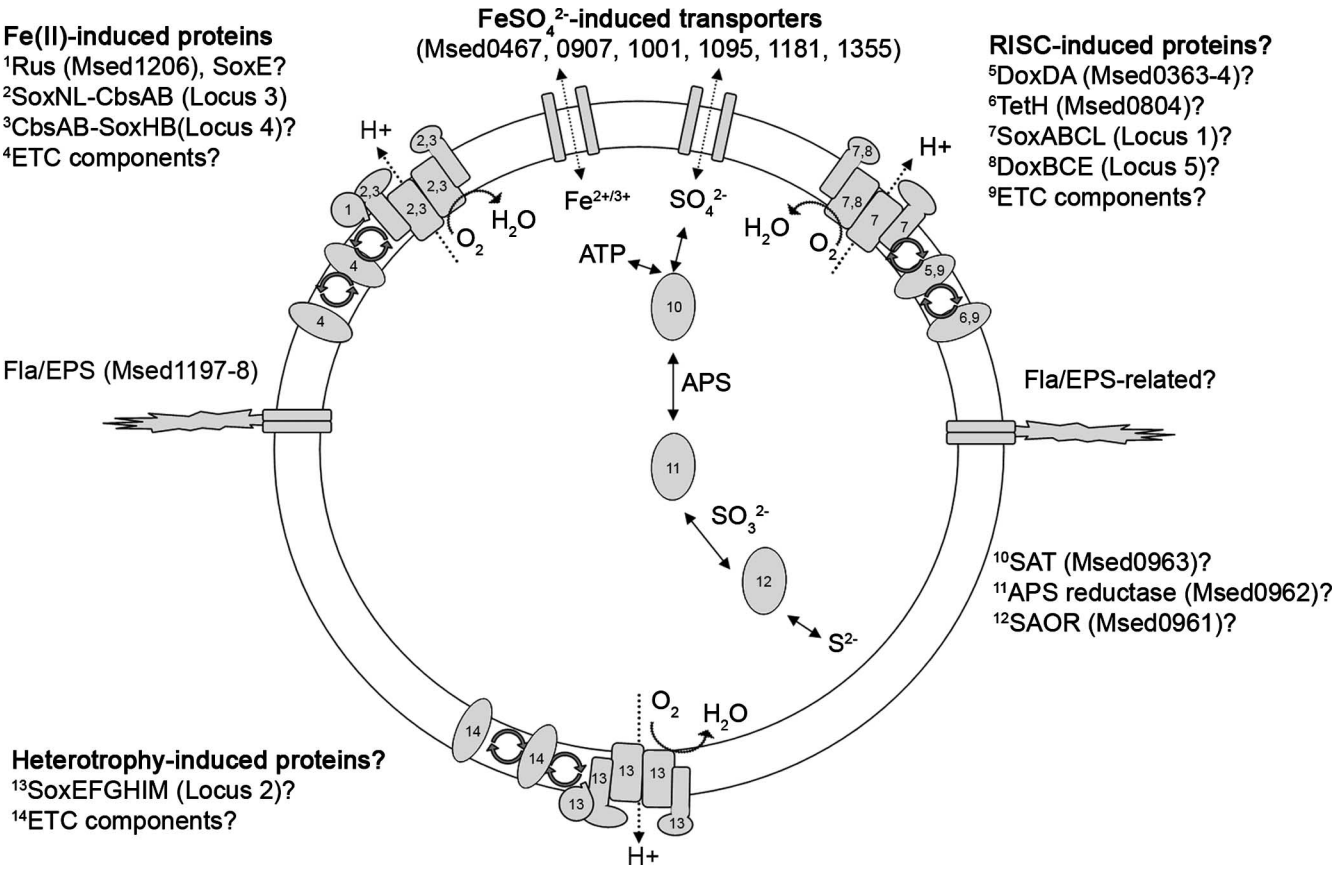

FIG. 6. Schematic summarizing Fe oxidation, sulfur metabolism, and adhesion components believed to be important to *M. sedula*'s biomining capacity. Elements of the schematic are linked to their annotations or putative functions by superscript numbers. Both genome sequence analysis and preliminary transcriptional profiling results ($FeSO_4$+YE versus YE) indicate that membrane-associated proteins have a prevalent role in biomining physiology.

(Msed1197 and -1198, Msed2104 and -2105, and Msed0650 and -0651). In the first two cases, *flaI*-like genes are annotated as encoding type II secretion system proteins, while their overlapping *flaJ*-like genes are annotated as encoding hypothetical proteins. In the last case, however, both genes are annotated as hypotheticals and share no overlap. Although all three FlaI-like proteins are closely related to the Msed1325 product, none of the three FlaJ-like proteins are similar to the Msed1324 product. Msed1198 has significant similarity to Msed2105, but neither is similar to Msed0651. Also of note is a prepilin/preflagellin peptidase gene located upstream of one of these FlaIJ pairs (Msed2090). With 237 amino acids and six predicted transmembrane helices, this FlaK-like sequence fits the characteristic size range and α-helix predictions for bacterial type II/IV systems (53).

Transcriptional response of *M. sedula* to $FeSO_4$. To assess whether specific aspects of bioinformatics analysis of *M. sedula* genome sequence have a physiological basis, transcriptional profiling using a whole-genome oligonucleotide microarray was pursued. The addition of $FeSO_4$ to a YE-supplemented medium triggered differential transcription of 88 genes (≥2.0-fold), or ~4% of the genome (Fig. 5; see Table S1 in the supplemental material). Of these, 53 were more highly transcribed in the presence of $FeSO_4$, including several *M. sedula* ORFs predicted to be involved with Fe oxidation, sulfur metabolism, and adhesion. Six ORFs, most with only a general "major facilitator superfamily" annotation, were up-regulated in the presence of $FeSO_4$+YE compared to YE (Msed0467, -0907, -1001, -1095, -1181, and -1355). Table 1 lists differentially transcribed ORFs predicted to be involved with Fe oxidation, sulfur metabolism, and adhesion, while Fig. 6 summarizes sequence-based predictions and preliminary transcriptome implications for these same three physiological functions. With respect to Fe oxidation, a putative rusticyanin (Msed1206), the locus 3 respiratory cluster (Msed0500 to Msed0504) expected to be up-regulated on Fe(II), and a unique putative quinol oxidase fusion protein (cytochrome *b* N-terminal and Rieske protein C-terminal domains) were highly transcribed in the presence of $FeSO_4$. Several *fox* genes of locus 4 (specifically Msed0477 to Msed0480) were also highly transcribed on $FeSO_4$, although levels in the presence of YE alone were at the upper end of the dynamic response range of the array. The exception to this was subunit I of the terminal oxidase (SoxB; Msed0484), which was more highly transcribed in the presence of $FeSO_4$+YE. The implied involvement of *M. sedula* locus 4 genes in Fe oxidation builds on previous reports on the closely related autotrophic biomining microorganism *S. metallicus* (5, 30), and the influence of a heterotrophic substrate (YE) com-

pared to $FeSO_4$ has not previously been investigated. ORFs potentially involved in sulfur metabolism (Msed0960 to Msed0963; CysGIHN-like sequences, respectively) were up-regulated in the presence of $FeSO_4$. With the addition of a sulfur compound in the +6 valence state, these ORFs, including the APS-SAT pair, may function in the reductive direction, reducing sulfate to sulfide. It is interesting that a cysteine synthase (CysM) gene-like ORF (Msed1607) was down-regulated on $FeSO_4$+YE. This may be an attempt to limit accumulation of cysteine, which could lead to Fenton reaction oxidative damage to DNA (70), although it is not immediately apparent how excess sulfide is alternatively processed. Additionally, Msed1197 and Msed1198, similar to genes for cytoplasmic ATPase and transmembrane subunits, were stimulated in the presence of $FeSO_4$ compared to YE alone. This FlaIJ pair was one of four Fla clusters predicted to be involved with adhesion, through either flagellum formation or EPS secretion. Although the three remaining Fla clusters may not function as predicted, it is also possible that their transcription has yet to be induced by the appropriate substrate. EPS production, composition, and properties have been observed to be a function of substrate in *A. ferrooxidans* (13, 24, 62). Finally, nearly half of the differentially transcribed ORFs in the YE-versus-YE+$FeSO_4$ contrast were annotated as encoding "hypothetical proteins" or "proteins of unknown function," indicating that novel proteins are involved in Fe oxidation metabolism in *M. sedula*. Efforts to understand Fe oxidation and other elements of *M. sedula* physiology using functional genomics approaches are under way.

Summary. Comparing genome sequences of extremely thermoacidophilic nonleachers, mesoacidophilic bioleachers, and *M. sedula* provides a number of preliminary insights into the genotype that supports high-temperature biomining. Such comparisons between *M. sedula* and genome-sequenced *Sulfolobales* indicate that the *fox* gene cluster, two putative versions of Rus, and TetH appear to be factors distinguishing thermoacidophilic bioleachers from nonbioleachers. However, it is still not clear whether bioleachers have acquired these genes or nonleachers have lost them (or their functionality). For example, the genome of the apparent nonleacher *S. solfataricus* encodes a protein similar to a putative Rus in *M. sedula* but is lacking a Rus protein signature and apparent Cu-binding ligands. *S. tokodaii* was recently demonstrated to have some degree of Fe oxidation capability and contains several *fox* genes (5), as well as a TetH, but is lacking a Rus-like sequence. Finally, the terminal oxidase components (locus 3) shown to be up-regulated on Fe(II) here, as well as in another study (36), were originally identified in the apparent nonleacher *S. acidocaldarius* (27). The differential transcription of significant numbers of hypothetical proteins in YE+$FeSO_4$-grown versus YE-grown *M. sedula* cells confirms there are many other proteins involved in Fe oxidation and/or sulfur metabolism which may help to further distinguish between bioleachers and nonleachers in the future.

The future success of the biomining industry will depend upon the performance of cellular biocatalysts. The availability of the *M. sedula* genome sequence has advanced both functional genomics and genetics efforts in this area. To understand performance, upcoming functional genomics studies will focus on *M. sedula* oxidation of RISCs and reduced Fe substrates and how these processes relate to cell adhesion to solid inorganic substrates. Functional genomics analyses can also help guide genetic tools in target selection. Genetic tools in development for *M. sedula* (Y. Maezato and P. Blum, unpublished data) will be important for examining and enhancing performance of pathways and metal-microbe interactions essential to biomining operations at elevated temperatures.

ACKNOWLEDGMENTS

We gratefully acknowledge the U.S. Department of Energy and the Joint Genome Institute for providing the genome sequence for *M. sedula*.

This work was supported in part by a grant from the U.S. National Science Foundation Biotechnology Program (no. BES-0317886). K.S.A. acknowledges support from an NIH T32 Biotechnology Traineeship.

REFERENCES

1. **Alber, B. E., M. Olinger, A. Rieder, D. Kockelkorn, B. Jobst, M. Hugler, and G. Fuchs.** 2006. Malonyl-coenyme A reductase in the modified 3-hydroxypropionate cycle for autotrophic carbon fixation in archaeal *Metallosphaera* and *Sulfolobus* spp. J. Bacteriol. **188:**8551–8559.
2. **Alvarez, S., and C. A. Jerez.** 2004. Copper ions stimulate polyphosphate degradation and phosphate efflux in *Acidithiobacillus ferrooxidans*. Appl. Environ. Microbiol. **70:**5177–5182.
3. **Barreto, M., E. Jedlicki, and D. S. Holmes.** 2005. Identification of a gene cluster for the formation of extracellular polysaccharide precursors in the chemolithoautotroph *Acidithiobacillus ferrooxidans*. Appl. Environ. Microbiol. **71:**2902–2909.
4. **Barrett, M. L., I. Harvey, M. Sundararajan, R. Surendran, J. F. Hall, M. J. Ellis, M. A. Hough, R. W. Strange, I. H. Hillier, and S. S. Hasnain.** 2006. Atomic resolution crystal structures, EXAFS, and quantum chemical studies of rusticyanin and its two mutants provide insight into its unusual properties. Biochemistry **45:**2927–2939.
5. **Bathe, S., and P. R. Norris.** 2007. Ferrous iron- and sulfur-induced genes in *Sulfolobus metallicus*. Appl. Environ. Microbiol. **73:**2491–2497.
6. **Bevilaqua, D., I. Diez-Perez, C. S. Fugivara, F. Sanz, A. V. Benedetti, and O. Garcia, Jr.** 2004. Oxidative dissolution of chalcopyrite by *Acidithiobacillus ferrooxidans* analyzed by electrochemical impedance spectroscopy and atomic force microscopy. Bioelectrochemistry **64:**79–84.
7. **Bruscella, P., C. Appia-Ayme, G. Levican, J. Ratouchniak, E. Jedlicki, D. S. Holmes, and V. Bonnefoy.** 2007. Differential expression of two bc1 complexes in the strict acidophilic chemolithoautotrophic bacterium *Acidithiobacillus ferrooxidans* suggests a model for their respective roles in iron or sulfur oxidation. Microbiology **153:**102–110.
8. **Buonfiglio, V., M. Polidoro, F. Soyer, P. Valenti, and J. Shively.** 1999. A novel gene encoding a sulfur-regulated outer membrane protein in *Thiobacillus ferrooxidans*. J. Biotechnol. **72:**85–93.
9. **Cardona, S. T., F. P. Chavez, and C. A. Jerez.** 2002. The exopolyphosphatase gene from *Sulfolobus solfataricus*: characterization of the first gene found to be involved in polyphosphate metabolism in archaea. Appl. Environ. Microbiol. **68:**4812–4819.
10. **Castresana, J., M. Lubben, and M. Saraste.** 1995. New archaebacterial genes coding for redox proteins: implications for the evolution of aerobic metabolism. J. Mol. Biol. **250:**202–210.
11. **Chen, Z. W., Y. Y. Liu, J. F. Wu, Q. She, C. Y. Jiang, and S. J. Liu.** 2007. Novel bacterial sulfur oxygenase reductases from bioreactors treating gold-bearing concentrates. Appl. Microbiol. Biotechnol. **74:**688–698.
12. **Clark, T. R., F. Baldi, and G. J. Olson.** 1993. Coal depyritization by the thermophilic archaeon *Metallosphaera sedula*. Appl. Environ. Microbiol. **59:**2375–2379.
13. **Devasia, P., K. A. Natarajan, D. N. Sathyanarayana, and G. R. Rao.** 1993. Surface chemistry of *Thiobacillus ferrooxidans* relevant to adhesion on mineral surfaces. Appl. Environ. Microbiol. **59:**4051–4055.
14. **Dixit, V., E. Bini, M. Drozda, and P. Blum.** 2004. Mercury inactivates transcription and the generalized transcription factor TFB in the archaeon *Sulfolobus solfataricus*. Antimicrob. Agents Chemother. **48:**1993–1999.
15. **Dopson, M., C. Baker-Austin, and P. L. Bond.** 2005. Analysis of differential protein expression during growth states of *Ferroplasma* strains and insights into electron transport for iron oxidation. Microbiology **151:**4127–4137.
16. **Dopson, M., C. Baker-Austin, P. R. Koppineedi, and P. L. Bond.** 2003. Growth in sulfidic mineral environments: metal resistance mechanisms in acidophilic micro-organisms. Microbiology **149:**1959–1970.
17. **Du Plessis, C. A., J. D. Batty, and D. W. Dew.** 2007. Commercial applications of thermophile bioleaching, p. 57–80. *In* D. E. Rawlings and D. B. Johnson (ed.), Biomining. Springer-Verlag, Berlin, Germany.
18. **Elbehti, A., G. Brasseur, and D. Lemesle-Meunier.** 2000. First evidence for

existence of an uphill electron transfer through the bc_1 and NADH-Q oxidoreductase complexes of the acidophilic obligate chemolithotrophic ferrous ion-oxidizing bacterium *Thiobacillus ferrooxidans*. J. Bacteriol. **182:**3602–3606.

19. **Ettema, T. J., A. B. Brinkman, P. P. Lamers, N. G. Kornet, W. M. de Vos, and J. van der Oost.** 2006. Molecular characterization of a conserved archaeal copper resistance (cop) gene cluster and its copper-responsive regulator in *Sulfolobus solfataricus* P2. Microbiology **152:**1969–1979.
20. **Friedmann, S., B. E. Alber, and G. Fuchs.** 2007. Properties of *R*-citramalyl-coenzyme A lyase and its role in the autotrophic 3-hydroxypropionate cycle of *Chloroflexus aurantiacus*. J. Bacteriol. **189:**2906–2914.
21. **Friedmann, S., B. E. Alber, and G. Fuchs.** 2006. Properties of succinyl-coenzyme A:D-citramalate coenzyme A transferase and its role in the autotrophic 3-hydroxypropionate cycle of *Chloroflexus aurantiacus*. J. Bacteriol. **188:**6460–6468.
22. **Friedmann, S., A. Steindorf, B. E. Alber, and G. Fuchs.** 2006. Properties of succinyl-coenzyme A:L-malate coenzyme A transferase and its role in the autotrophic 3-hydroxypropionate cycle of *Chloroflexus aurantiacus*. J. Bacteriol. **188:**2646–2655.
23. **Gehrke, T., R. Hallmann, K. Kinzler, and W. Sand.** 2001. The EPS of *Acidithiobacillus ferrooxidans*—a model for structure-function relationships of attached bacteria and their physiology. Water Sci. Technol. **43:**159–167.
24. **Gehrke, T., J. Telegdi, D. Thierry, and W. Sand.** 1998. Importance of extracellular polymeric substances from *Thiobacillus ferrooxidans* for bioleaching. Appl. Environ. Microbiol. **64:**2743–2747.
25. **Giri, A. V., S. Anishetty, and P. Gautam.** 2004. Functionally specified protein signatures distinctive for each of the different blue copper proteins. BMC Bioinformatics **5:**127.
26. **Haseltine, C., R. Montalvo-Rodriguez, E. Bini, A. Carl, and P. Blum.** 1999. Coordinate transcriptional control in the hyperthermophilic archaeon *Sulfolobus solfataricus*. J. Bacteriol. **181:**3920–3927.
27. **Hiller, A., T. Henninger, G. Schafer, and C. L. Schmidt.** 2003. New genes encoding subunits of a cytochrome bc1-analogous complex in the respiratory chain of the hyperthermoacidophilic crenarchaeon *Sulfolobus acidocaldarius*. J. Bioenerg. Biomembr. **35:**121–131.
28. **Holmes, D. S., and V. Bonnefoy.** 2007. Genetic and bioinformatic insights into iron and sulfur oxidation mechanisms of bioleaching organisms, p. 281–307. *In* D. E. Rawlings and D. B. Johnson (ed.), Biomining. Springer-Verlag, Berlin, Germany.
29. **Huber, G., C. Spinnler, A. Gambacorta, and K. O. Stetter.** 1989. *Metallosphaera sedula* gen. and sp. nov. represents a new genus of aerobic, metal-mobilizing, thermoacidophilic archaebacteria. Syst. Appl. Microbiol. **12:**38–47.
30. **Huber, G., and K. O. Stetter.** 1991. *Sulfolobus metallicus*, sp. nov., a novel strictly chemolithoautotrophic thermophilic archaeal species of metal-mobilizers. Syst. Appl. Microbiol. **14:**372–378.
31. **Hugler, M., and G. Fuchs.** 2005. Assaying for the 3-hydroxypropionate cycle of carbon fixation. Methods Enzymol. **397:**212–221.
32. **Hugler, M., H. Huber, K. O. Stetter, and G. Fuchs.** 2003. Autotrophic CO_2 fixation pathways in archaea (Crenarchaeota). Arch. Microbiol. **179:**160–173.
33. **Hugler, M., R. S. Krieger, M. Jahn, and G. Fuchs.** 2003. Characterization of acetyl-CoA/propionyl-CoA carboxylase in *Metallosphaera sedula*. Carboxylating enzyme in the 3-hydroxypropionate cycle for autotrophic carbon fixation. Eur. J. Biochem. **270:**736–744.
34. **Ishii, M., S. Chuakrut, H. Arai, and Y. Igarashi.** 2004. Occurrence, biochemistry and possible biotechnological application of the 3-hydroxypropionate cycle. Appl. Microbiol. Biotechnol. **64:**605–610.
35. **Kanao, T., K. Kamimura, and T. Sugio.** 2007. Identification of a gene encoding a tetrathionate hydrolase in *Acidithiobacillus ferrooxidans*. J. Biotechnol. **132:**16–22.
36. **Kappler, U., L. I. Sly, and A. G. McEwan.** 2005. Respiratory gene clusters of *Metallosphaera sedula*—differential expression and transcriptional organization. Microbiology **151:**35–43.
37. **Kletzin, A.** 1989. Coupled enzymatic production of sulfite, thiosulfate, and hydrogen sulfide from sulfur: purification and properties of a sulfur oxygenase reductase from the facultatively anaerobic archaebacterium *Desulfurolobus ambivalens*. J. Bacteriol. **171:**1638–1643.
38. **Kletzin, A., T. Urich, F. Muller, T. M. Bandeiras, and C. M. Gomes.** 2004. Dissimilatory oxidation and reduction of elemental sulfur in thermophilic archaea. J. Bioenerg. Biomembr. **36:**77–91.
39. **Komorowski, L., W. Verheyen, and G. Schafer.** 2002. The archaeal respiratory supercomplex SoxM from *S. acidocaldarius* combines features of quinole and cytochrome c oxidases. Biol. Chem. **383:**1791–1799.
40. **Lin, W. S., T. Cunneen, and C. Y. Lee.** 1994. Sequence analysis and molecular characterization of genes required for the biosynthesis of type 1 capsular polysaccharide in *Staphylococcus aureus*. J. Bacteriol. **176:**7005–7016.
41. **Lubben, M., S. Arnaud, J. Castresana, A. Warne, S. P. Albracht, and M. Saraste.** 1994. A second terminal oxidase in *Sulfolobus acidocaldarius*. Eur. J. Biochem. **224:**151–159.
42. **Meister, M., S. Saum, B. E. Alber, and G. Fuchs.** 2005. L-Malyl-coenzyme A/β-methylmalyl-coenzyme A lyase is involved in acetate assimilation of the isocitrate lyase-negative bacterium *Rhodobacter capsulatus*. J. Bacteriol. **187:**1415–1425.
43. **Menendez, C., Z. Bauer, H. Huber, N. Gad'on, K. O. Stetter, and G. Fuchs.** 1999. Presence of acetyl coenzyme A (CoA) carboxylase and propionyl-CoA carboxylase in autotrophic *Crenarchaeota* and indication for operation of a 3-hydroxypropionate cycle in autotrophic carbon fixation. J. Bacteriol. **181:**1088–1098.
44. **Morin, D. H. R., and P. D'Hugues.** 2007. Bioleaching of a cobalt-containing pyrite in stirred reactors: a case study from laboratory scale to industrial application, p. 35–55. *In* D. E. Rawlings and D. B. Johnson (ed.), Biomining. Springer-Verlag, Berlin, Germany.
45. **Muller, F. H., T. M. Bandeiras, T. Urich, M. Teixeira, C. M. Gomes, and A. Kletzin.** 2004. Coupling of the pathway of sulphur oxidation to dioxygen reduction: characterization of a novel membrane-bound thiosulphate:quinone oxidoreductase. Mol. Microbiol. **53:**1147–1160.
46. **Nather, D. J., R. Rachel, G. Wanner, and R. Wirth.** 2006. Flagella of *Pyrococcus furiosus*: multifunctional organelles, made for swimming, adhesion to various surfaces, and cell-cell contacts. J. Bacteriol. **188:**6915–6923.
47. **Nemati, M., J. Lowenadler, and S. T. Harrison.** 2000. Particle size effects in bioleaching of pyrite by acidophilic thermophile *Sulfolobus metallicus* (BC). Appl. Microbiol. Biotechnol. **53:**173–179.
48. **Nies, D. H.** 2003. Efflux-mediated heavy metal resistance in prokaryotes. FEMS Microbiol. Rev. **27:**313–339.
49. **Norris, P. R.** 2007. Acidophile diversity in mineral sulfide oxidation, p. 199–216. *In* D. E. Rawlings and D. B. Johnson (ed.), Biomining. Springer-Verlag, Berlin, Germany.
50. **Norris, P. R., N. P. Burton, and N. A. Foulis.** 2000. Acidophiles in bioreactor mineral processing. Extremophiles **4:**71–76.
51. **Ohmura, N., K. Kitamura, and H. Saiki.** 1993. Selective adhesion of *Thiobacillus ferrooxidans* to pyrite. Appl. Environ. Microbiol. **59:**4044–4050.
52. **Olson, G. J., J. A. Brierley, and C. L. Brierley.** 2003. Bioleaching review part B: progress in bioleaching: applications of microbial processes by the minerals industries. Appl. Microbiol. Biotechnol. **63:**249–257.
53. **Peabody, C. R., Y. J. Chung, M. R. Yen, D. Vidal-Ingigliardi, A. P. Pugsley, and M. H. Saier, Jr.** 2003. Type II protein secretion and its relationship to bacterial type IV pili and archaeal flagella. Microbiology **149:**3051–3072.
54. **Purschke, W. G., C. L. Schmidt, A. Petersen, and G. Schafer.** 1997. The terminal quinol oxidase of the hyperthermophilic archaeon *Acidianus ambivalens* exhibits a novel subunit structure and gene organization. J. Bacteriol. **179:**1344–1353.
55. **Ramirez, P., N. Guiliani, L. Valenzuela, S. Beard, and C. A. Jerez.** 2004. Differential protein expression during growth of *Acidithiobacillus ferrooxidans* on ferrous iron, sulfur compounds, or metal sulfides. Appl. Environ. Microbiol. **70:**4491–4498.
56. **Rawlings, D. E.** 2005. Characteristics and adaptability of iron- and sulfur-oxidizing microorganisms used for the recovery of metals from minerals and their concentrates. Microb. Cell Fact. **4:**13.
57. **Rawlings, D. E., D. Dew, and C. du Plessis.** 2003. Biomineralization of metal-containing ores and concentrates. Trends Biotechnol. **21:**38–44.
58. **Remonsellez, F., A. Orell, and C. A. Jerez.** 2006. Copper tolerance of the thermoacidophilic archaeon *Sulfolobus metallicus*: possible role of polyphosphate metabolism. Microbiology **152:**59–66.
59. **Rohwerder, T., T. Gehrke, K. Kinzler, and W. Sand.** 2003. Bioleaching review part A: progress in bioleaching: fundamentals and mechanisms of bacterial metal sulfide oxidation. Appl. Microbiol. Biotechnol. **63:**239–248.
60. **Rolfsmeier, M., and P. Blum.** 1995. Purification and characterization of a maltase from the extremely thermophilic crenarchaeote *Sulfolobus solfataricus*. J. Bacteriol. **177:**482–485.
61. **Rzhepishevska, O. I., J. Valdes, L. Marcinkeviciene, C. A. Gallardo, R. Meskys, V. Bonnefoy, D. S. Holmes, and M. Dopson.** 2007. Regulation of a novel *Acidithiobacillus caldus* gene cluster involved in reduced inorganic sulfur compound metabolism. Appl. Environ. Microbiol. **73:**7367–7372.
62. **Sand, W., and T. Gehrke.** 2006. Extracellular polymeric substances mediate bioleaching/biocorrosion via interfacial processes involving iron(III) ions and acidophilic bacteria. Res. Microbiol. **157:**49–56.
63. **Schelert, J., V. Dixit, V. Hoang, J. Simbahan, M. Drozda, and P. Blum.** 2004. Occurrence and characterization of mercury resistance in the hyperthermophilic archaeon *Sulfolobus solfataricus* by use of gene disruption. J. Bacteriol. **186:**427–437.
64. **Schelert, J., M. Drozda, V. Dixit, A. Dillman, and P. Blum.** 2006. Regulation of mercury resistance in the crenarchaeote *Sulfolobus solfataricus*. J. Bacteriol. **188:**7141–7150.
65. **Schoepp-Cothenet, B., M. Schutz, F. Baymann, M. Brugna, W. Nitschke, H. Myllykallio, and C. Schmidt.** 2001. The membrane-extrinsic domain of cytochrome b(558/566) from the archaeon *Sulfolobus acidocaldarius* performs pivoting movements with respect to the membrane surface. FEBS Lett. **487:**372–376.
66. **Skerker, J. M., and H. C. Berg.** 2001. Direct observation of extension and retraction of type IV pili. Proc. Natl. Acad. Sci. USA **98:**6901–6904.
67. **Strauss, G., and G. Fuchs.** 1993. Enzymes of a novel autotrophic CO_2 fixation pathway in the phototrophic bacterium *Chloroflexus aurantiacus*, the 3-hydroxypropionate cycle. Eur. J. Biochem. **215:**633–643.

68. **Tyson, G. W., J. Chapman, P. Hugenholtz, E. E. Allen, R. J. Ram, P. M. Richardson, V. V. Solovyev, E. M. Rubin, D. S. Rokhsar, and J. F. Banfield.** 2004. Community structure and metabolism through reconstruction of microbial genomes from the environment. Nature **428:**37–43.
69. **Urich, T., C. M. Gomes, A. Kletzin, and C. Frazao.** 2006. X-ray structure of a self-compartmentalizing sulfur cycle metalloenzyme. Science **311:**996–1000.
70. **Valdes, J., F. Veloso, E. Jedlicki, and D. Holmes.** 2003. Metabolic reconstruction of sulfur assimilation in the extremophile *Acidithiobacillus ferrooxidans* based on genome analysis. BMC Genomics **4:**51.
71. **van Aswegen, P. C., J. van Niekerk, and W. Olivier.** 2007. The BIOX(TM) process for the treatment of refractory gold concentrates, p. 1–33. *In* D. E. Rawlings and D. B. Johnson (ed.), Biomining. Springer-Verlag, Berlin, Germany.
72. **Yarzabal, A., C. Appia-Ayme, J. Ratouchniak, and V. Bonnefoy.** 2004. Regulation of the expression of the *Acidithiobacillus ferrooxidans* rus operon encoding two cytochromes c, a cytochrome oxidase and rusticyanin. Microbiology **150:**2113–2123.
73. **Yildiz, F. H., and G. K. Schoolnik.** 1999. *Vibrio cholerae* O1 El Tor: identification of a gene cluster required for the rugose colony type, exopolysaccharide production, chlorine resistance, and biofilm formation. Proc. Natl. Acad. Sci. USA **96:**4028–4033.
74. **Yu, Z., E. B. Lansdon, I. H. Segel, and A. J. Fisher.** 2007. Crystal structure of the bifunctional ATP sulfurylase-APS kinase from the chemolithotrophic thermophile *Aquifex aeolicus*. J. Mol. Biol. **365:**732–743.
75. **Zahringer, U., H. Moll, T. Hettmann, Y. A. Knirel, and G. Schafer.** 2000. Cytochrome b558/566 from the archaeon *Sulfolobus acidocaldarius* has a unique Asn-linked highly branched hexasaccharide chain containing 6-sulfoquinovose. Eur. J. Biochem. **267:**4144–4149.
76. **Zeng, J., M. Geng, Y. Liu, L. Xia, J. Liu, and G. Qiu.** 2007. The sulfhydryl group of Cys138 of rusticyanin from *Acidithiobacillus ferrooxidans* is crucial for copper binding. Biochim. Biophys. Acta **1774:**519–525.

Supplementary Table 1: ORFs in *Metallosphaera sedula* differentially expressed 2.0-fold (log2 fold=1.0) or higher upon addition of ferrous sulfate to YE-supplemented medium

YE = yeast extract supplemented media; YEF = yeast extract + $FeSO_4 \cdot 7H_2O$ supplemented media.

Gene ID	Lsm[a] YE	Lsm[a] YEF	Log2 fold change = (YE) -(YEF)	-log10 (p-value) for (YE) -(YEF)	GenBank Annotation (19Aug2007)	Auernik et al. Annotation Notes/Comments
Msed0012	0.769	-0.192	0.960	2.557	Prephenate dehydratase	
Msed0028	1.595	0.626	0.969	3.099	ribosomal protein L24E	
Msed0062	1.683	0.604	1.079	4.479	RNA polymerase Rpb4	
Msed0149	-1.821	1.675	-3.496	13.316	exonuclease of the beta-lactamase fold involved in RNA processing-like protein	hypothetical exonuclease
Msed0161	1.335	0.379	0.956	2.650	hypothetical protein Msed_0161	hypothetical protein
Msed0203	0.670	-0.449	1.118	4.365	ribosomal protein L40e	50S ribosomal protein L40e
Msed0236	2.269	0.986	1.283	4.559	sugar isomerase (SIS)	hypothetical D-arabino-3-hexulose-6-phosphate isomerase
Msed0242	0.308	1.411	-1.103	7.341	peptidase M48, Ste24p	hypothetical Zn-dependent protease
Msed0267	0.251	1.373	-1.122	1.685	AMP-dependent synthetase and ligase	putative acetyl-CoA synthetase
Msed0307	3.131	4.136	-1.005	5.510	pyruvate ferredoxin/flavodoxin oxidoreductase, delta subunit	
Msed0327	-1.206	0.140	-1.345	4.738	hypothetical protein Msed_0327	
Msed0328	2.922	1.763	1.160	3.837	hypothetical protein Msed_0328	
Msed0341	1.248	3.498	-2.249	7.392	hypothetical protein Msed_0341	
Msed0347	1.482	2.788	-1.306	9.782	hypothetical protein Msed_0347	
Msed0380	0.719	2.044	-1.324	5.656	hypothetical protein Msed_0380	
Msed0429	-1.114	0.320	-1.434	2.985	hypothetical protein Msed_0429	
Msed0450	1.529	0.532	0.997	3.204	protein of unknown function DUF1291	
Msed0456	1.967	0.985	0.981	3.333	hypothetical protein Msed_0456	
Msed0458	1.739	2.914	-1.174	5.320	hypothetical protein Msed_0458	bacterial adhesion domain
Msed0467	-1.629	-0.170	-1.459	8.036	major facilitator superfamily MFS_1	
Msed0478	4.463	2.754	1.709	7.290	hypothetical protein Msed_0478	cytochrome b558-566
Msed0479	4.402	1.957	2.446	8.088	hypothetical protein Msed_0479	hypothetical membrane/ extracellular protein
Msed0480	4.773	2.858	1.915	10.479	cytochrome c oxidase, subunit II	quinol oxidase (subunit 2)

Msed0482	2.370	1.299	1.071	3.461	hypothetical protein Msed_0482	hypothetical protein
Msed0500	0.890	2.482	-1.591	4.070	Cytochrome b/b6, N-terminal domain	quinol oxidase (cyt b subunit)
Msed0504	0.802	1.820	-1.018	1.671	hypothetical protein Msed_0504	cytochrome b558-566 (subunit A)
Msed0507	-0.506	1.329	-1.835	5.612	pyruvate/ketoisovalerate oxidoreductase, gamma subunit	
Msed0508	-0.143	1.728	-1.870	5.838	pyruvate ferredoxin/flavodoxin oxidoreductase, delta subunit	
Msed0509	-1.048	0.952	-2.000	5.462	pyruvate flavodoxin/ferredoxin oxidoreductase domain protein	
Msed0510	0.276	2.281	-2.006	6.278	thiamine pyrophosphate enzyme domain protein TPP-binding	
Msed0511	-1.224	0.439	-1.663	6.035	Radical SAM domain protein	
Msed0512	-1.518	0.112	-1.630	4.339	Radical SAM domain protein	
Msed0513	-1.888	0.146	-2.034	6.475	beta-lactamase domain protein	
Msed0514	-1.627	0.292	-1.919	5.978	peptidase U32	
Msed0515	-2.244	0.237	-2.481	9.397	Radical SAM domain protein	
Msed0516	2.259	3.222	-0.963	7.308	hypothetical protein Msed_0516	conserved hypothetical protein
Msed0518	-0.583	2.868	-3.451	11.295	hypothetical protein Msed_0518	
Msed0529	-0.350	0.812	-1.162	4.510	hypothetical protein Msed_0529	
Msed0535	-2.058	0.317	-2.375	12.462	hypothetical protein Msed_0535	
Msed0562	0.723	-0.517	1.240	3.098	hypothetical protein Msed_0562	
Msed0578	1.621	0.498	1.123	3.269	hypothetical protein Msed_0578	
Msed0579	4.622	3.099	1.523	5.043	hypothetical protein Msed_0579	
Msed0621	1.367	0.137	1.230	4.199	CopG domain protein DNA-binding domain protein	
Msed0705	0.590	1.954	-1.364	4.682	peptidase S8 and S53, subtilisin, kexin, sedolisin	
Msed0960	-2.956	-1.619	-1.337	9.291	Uroporphyrin-III C/tetrapyrrole (Corrin/Porphyrin) methyltransferase	uroporphyrin-III C-methyltransferase
Msed0961	-2.439	-0.876	-1.564	8.453	nitrite and sulphite reductase 4Fe-4S region	sulfite reductase
Msed0962	-0.647	1.033	-1.680	5.860	adenylylsulfate reductase, thioredoxin dependent	putative adenosine phosphosulfate (APS) reductase
Msed1001	-2.080	-1.034	-1.046	9.129	major facilitator superfamily MFS_1	
Msed1003	-0.237	0.806	-1.043	3.789	Methyltransferase type 11	
Msed1020	-2.357	-0.671	-1.687	7.366	hypothetical protein Msed_1020	
Msed1095	-1.780	-0.655	-1.125	4.453	major facilitator superfamily MFS_1	

Msed1181	-1.926	-0.525	-1.402	7.924	extracellular solute-binding protein, family 1	
Msed1189	1.453	4.079	-2.626	7.487	hypothetical protein Msed_1189	
Msed1191	-1.006	1.087	-2.093	4.014	Rieske (2Fe-2S) domain protein	fused cyt b556 and Rieske protein
Msed1193	-0.138	4.434	-4.572	14.836	hypothetical protein Msed_1193	archaeal flagellin / bacterial Type II/IV N-terminal domain protein
Msed1194	-0.350	3.651	-4.000	13.615	hypothetical protein Msed_1194	hypothetical membrane/extracellular protein
Msed1195	-1.855	2.279	-4.134	10.826	hypothetical protein Msed_1195	hypothetical membrane/extracellular protein
Msed1196	-0.939	3.493	-4.432	13.746	hypothetical protein Msed_1196	hypothetical membrane/extracellular protein
Msed1197	-1.453	2.179	-3.632	11.369	type II secretion system protein E	Type II/IV secretion system protein (ATP-binding subunit)
Msed1198	-0.486	2.094	-2.580	6.271	type II secretion system protein	Type II/IV/flagellar subunit (FlaJ)
Msed1205	0.324	-0.702	1.026	3.575	hypothetical protein Msed_1205	
Msed1273	2.639	1.630	1.009	2.977	hypothetical protein Msed_1273	
Msed1355	-0.750	1.346	-2.095	9.903	major facilitator superfamily MFS_1	
Msed1370	2.829	3.802	-0.973	3.421	hypothetical protein Msed_1370	
Msed1403	0.641	-0.382	1.023	5.016	putative endoribonuclease L-PSP	
Msed1407	0.276	-0.817	1.094	2.242	hypothetical protein Msed_1407	
Msed1409	0.827	-0.168	0.995	2.079	hypothetical protein Msed_1409	
Msed1455	1.953	0.985	0.968	2.102	amino acid permease-associated region	amino acid transporter / permease
Msed1461	0.658	1.761	-1.103	4.209	hypothetical protein Msed_1461	conserved hypothetical membrane protein
Msed1520	-1.260	-0.294	-0.966	2.380	hypothetical protein Msed_1520	conserved hypothetical protein
Msed1528	0.875	1.829	-0.953	4.175	protein of unknown function DUF214	hypothetical ABC transporter (membrane component)
Msed1529	-0.317	0.857	-1.174	7.006	hypothetical protein Msed_1529	conserved membrane protein
Msed1578	1.868	0.840	1.028	3.970	purine or other phosphorylase, family 1	S-methyl-5-thioadenosine phosphorylase
Msed1580	2.803	1.132	1.671	10.465	hypothetical protein Msed_1580	conserved hypothetical protein
Msed1607	1.079	0.005	1.073	3.651	Pyridoxal-5'-phosphate-dependent enzyme, beta subunit	hypothetical cysteine synthase A
Msed1612	0.316	-0.871	1.187	4.364	glutamine synthetase, type I	glutamine synthetase
Msed1636	3.694	2.695	0.999	2.799	ribosomal protein L10	50S / 60S acidic ribosomal protein

						L10
Msed1668	0.941	2.169	-1.228	5.508	Phosphopyruvate hydratase	enolase
Msed1732	3.916	2.846	1.070	3.163	hypothetical protein Msed_1732	conserved hypothetical protein
Msed1865	2.881	1.910	0.971	1.589	ribosomal protein L10E	50S ribosomal protein L10E
Msed1892	0.640	-0.344	0.984	2.195	hypothetical protein Msed_1892	conserved hypothetical protein
Msed1910	2.467	1.423	1.045	2.116	hypothetical protein Msed_1910	conserved hypothetical protein
Msed1985	3.301	2.099	1.201	2.536	hypothetical protein Msed_1985	conserved hypothetical protein
Msed2028	1.838	0.766	1.072	2.815	transcriptional regulator, AbrB family	hypothetical vapB antitoxin
Msed2132	4.404	3.240	1.164	3.845	ribosomal protein L7Ae/L30e/S12e/Gadd45	50S ribosomal protein L7Ae
Msed2164	1.505	5.022	-3.517	17.012	protein of unknown function DUF87	hypothetical ATP-binding protein
Msed2211	2.431	1.368	1.062	3.140	RNA polymerase Rbp10	
Msed2252	2.819	1.827	0.992	2.719	ribosomal protein L37e	

[a] Lsm (least squares mean) denotes normalized log2 transcription levels such that lsm = 0 represents the average mRNA transcription level for the dataset using a mixed ANOVA model, with -3.5 and 5.1 being the normalized dataset minimum and maximum values (not shown).

[b] For reference, significance values of 1.3, 4.3, and 9.3 correlate to p-values of 0.05, 5×10^{-5}, and 5×10^{-10}, respectively.